COMPUTATIONAL ANALYSIS AND RE-DESIGN OF A WING-STRAKE COMBINATION

Yngve C-J. Sedin, Ingemar Persson, Mattias Sillen
Saab Aerosystems
SE-581 88 LINKÖPING, Sweden
(Email: yngve.sedin@saab.se)

Abstract

Wind tunnel testing of a swept wing-strake aircraft configuration revealed local losses in aerodynamic lift and lift-slope at high angles of attack. 3D Navier-Stokes analysis indicated local disturbances. A re-design operation was initiated to improve on wing characteristics. Conditions were set for holding wing plan-form and shape of strake intact making changes to the outboard wing keeping volume and thickness fixed.

The re-design procedure was set up using equivalent 2D calculations for quick guidelines to local leading edge modifications. 3D Navier-Stokes analysis was performed 'en masse' and calculations were done on a computer cluster.

Several modifications were tried and improvements in aerodynamic characteristics were achieved. Local loss of lift with sudden drag-increase seems related to breakdown of in-plane leading edge suction. Leading edge modifications and changed wing twist delayed this process, gradually smearing it with angle of attack yielding smoothed lift and reduced drag.

1 Introduction

The upward turning cost spiral of development of military equipment, operation and training, is a strong driver for combined multipurpose solutions achieving cost effectiveness. Basic flight and advanced tactical training could overall be combined into one successive training system. During year 2000 a Swedish national research program (NFFP-379) was initiated to see how a cost effective trainer should look like and fit into a future scenario ranging from basic training up to advanced tactical. The technology level should match modern systems up to a reasonable degree of functionality and to lower cost than todays.

During the NFFP-program an aircraft configuration, Ref [5], was selected. The outline was tandem seated having a swept wing and aft-tail combination. The shoulder-mounted wing was provided with an inboard strake. The wing span was about 8 meters and the take-off weight around 5000 kg. The configuration was designed for low up to transonic speeds.

Wind tunnel tests were performed in low and high speed at FFA (The Aeronautical Research Institute of Sweden, now within FOI, the Swedish Defense Research Agency).

Test results gave rise to questions about improvements of aerodynamic wing characteristics at high angles of attack. Experimental data indicated local loss of lift and degrading lift slope well before maximum lift. This is not so uncommon for this type of swept wing having fairly thin or sharp leading edges.

A limited design study, Ref [6], was initiated. It turned out that a re-design of the outboard wing leading edge ahead of 15% chord with slightly changed wing twist improved on characteristics.

2 General Background

2.1 Background of Study

The subsonic trainer configuration, named FU518TA, is shown in Fig 1. It has a 30.8-degree leading edge swept wing with an inboard strake. The relative wing thickness is ranging from inboard 8% to outboard 6 %. Although

fairly thick, compared to classic supersonic fighters, its original leading edge shape was quite thin with a relatively small radius.

Fig 1. Configuration FU518TA.

A wind tunnel model was tested in the high-speed tunnel T1500 at FFA from Reynolds number 3.4 million up to about 7 million. The Mach number range was within 0.22-0.95. In low speed the lift coefficient CL versus angle of attack (AoA) was measured as shown in Fig 2.

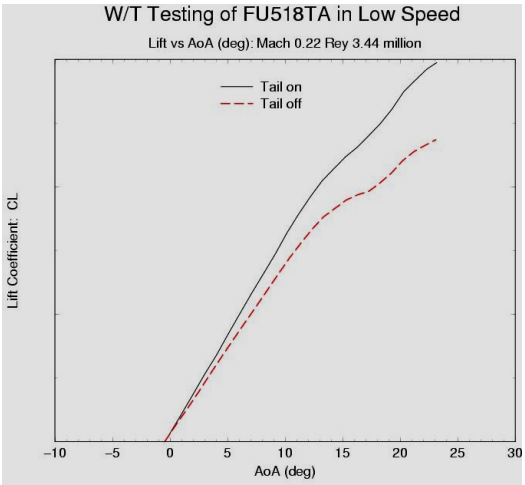

Fig 2. CL versus Angle of Attack (AoA) measured in T1500 with tail on and tail off.

Both tail-on and tail-off show the same type of behavior. Both have a local shallow bucket of loss of lift in the AoA range between 12 and 20 degrees. Degradation in lift slope starts around AoA 10-12 degrees at the same time as the leading edge suction is beginning to decrease, see the tangential force coefficient CT in Fig 3.

Altogether this gave rise to some concern regarding aerodynamic wing characteristics as it occurred well before CL-max. A limited computational study was decided to analyze the phenomenon and to suggest re-design measures to improve on aerodynamic characteristics. Presumably, the degradation of leading edge suction plays an important role.

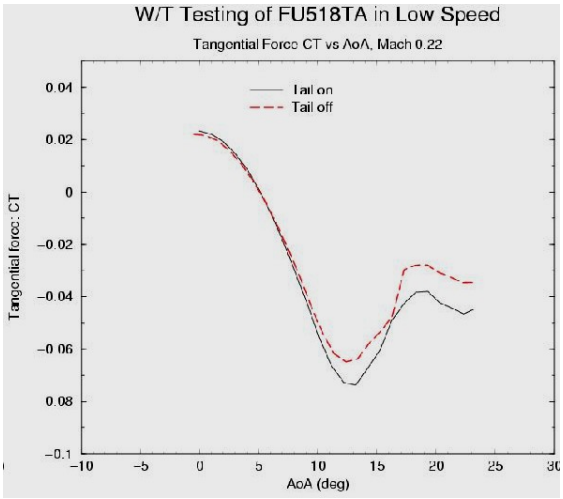

Fig 3. CT versus AoA measured in T1500 with tail on and tail off.

Local degradation of lift is not so uncommon for this type of wing-strake combination having thin fairly sharp leading edges. In the present case the local disturbance on lift is fairly smooth. However, it can be more sudden and ‘glitch-like’ as shown in Ref [1] with the NLR tested TWIG model.

2.2 Leading Edge Suction and ‘Glitches’

In Ref [1] a generic swept wing-strake model (Fig 4) was wind tunnel tested at high angles of attack in the Mach range 0.5-0.8.

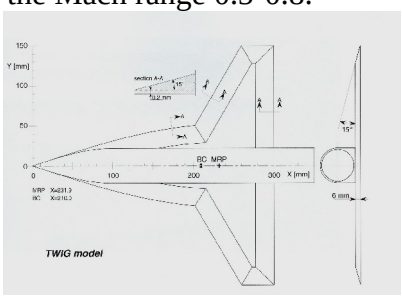

Fig 4. NLR TWIG wind tunnel model.

Wing and strake were thin plates with beveled edges giving sharp corners and leading edges inviting local separation and lift-off of vortices.

Measurements indicated a step-like loss of lift with an almost parallel shear of lift just above an AoA of about 10-12 degrees. The 'glitch-like' behavior of lift became more pronounced with higher Mach numbers. However, it was clearly visible at Mach 0.5. In spite of the thin forward facing leading edge front area, the integrated effect seems to be the notable mechanism of sudden loss of leading edge suction demonstrated in Fig 5. The tangential force CT is there plotted against the normal force CN. The loss of suction (-CT) is at CN=0.9 inflicting on CL due to corresponding projection loss of the CT component.

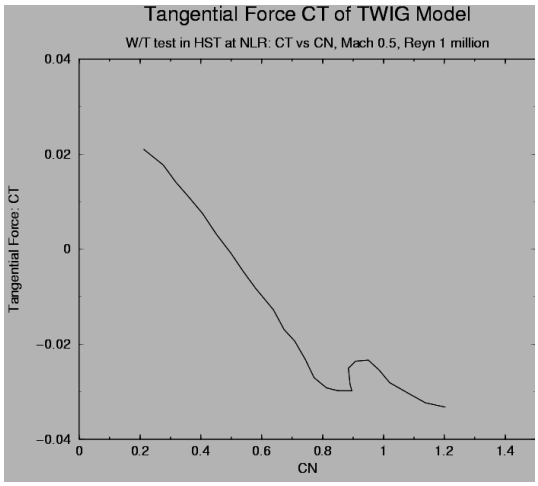

Fig 5. TWIG tangential force CT versus normal force CN at Mach 0.5.

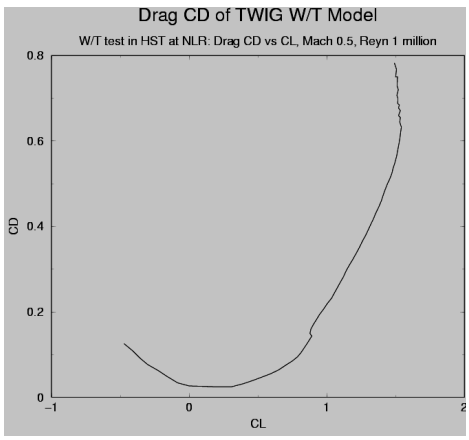

Fig 6. TWIG lift-dependent drag, Mach 0.5.

The sudden loss of suction (Fig 5) has a strong impact on lift-dependent drag as can be seen in Fig 6. The substructure of the leading edge flow is quickly changing from one state to the other, creating local glitches in lift and drag.

One could speculate whether transonic flow is primarily involved at the leading edge when the flow rapidly is expanding around the nose at high angles of attack. However, it seems more likely that centrifugal forces do not match the available out-leading normal pressure gradient turning the flow around the leading edge of high curvature. Hence, flow lift-off will occur with local bubble cavities and separation of free vortices, suddenly changing the flow and reducing suction forces. It is a subtle mechanism where pressure and shape are inter-related and viscid and in-viscid interactions take place. In transonic this will be even more complex with emerging shock waves retarding the flow with adverse pressure gradients.

2.3 Computational Model Approaches

It should be possible to optimize wing leading edge shapes to locally meet the on-coming flow better, hence reducing 'glitch-like' behaviors. This would maintain nose suction longer and smearing the breakdown process.

To quickly come to analysis and re-design, 3D Navier-Stokes calculations were advocated for analysis on the wing attached to a simplified fuselage. The latter was to facilitate grid generation and shorten turnaround time. Hence, the wing was fitted to a cylindrical body having an ogive nose, see Fig 7. With this geometry, the baseline wing called V0 was computed at Mach 0.22. CL-data was qualitatively corrected with respect to different wing incidence and boat tail for purpose of comparison. Data was compared with wind tunnel measurements of the full configuration FU518TA in Fig 8.

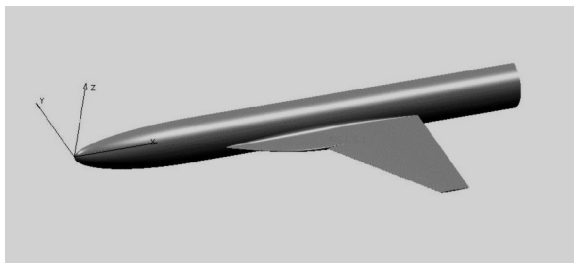

Fig 7. Wing-body model for 3D flow analysis.

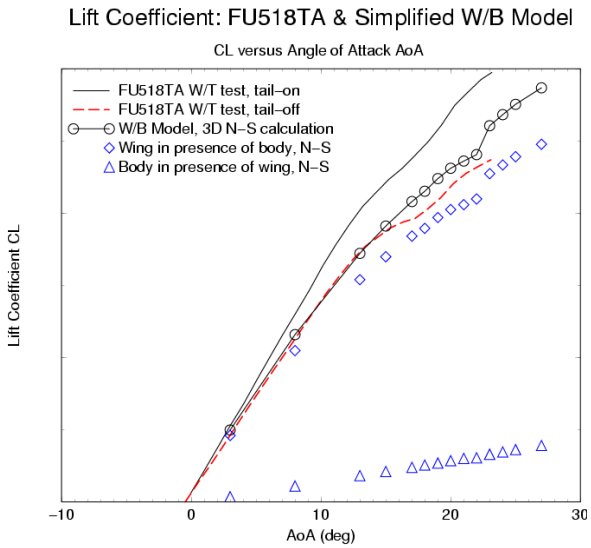

Fig 8. CL comparison between corrected Navier-Stokes calculations and FU518TA data.

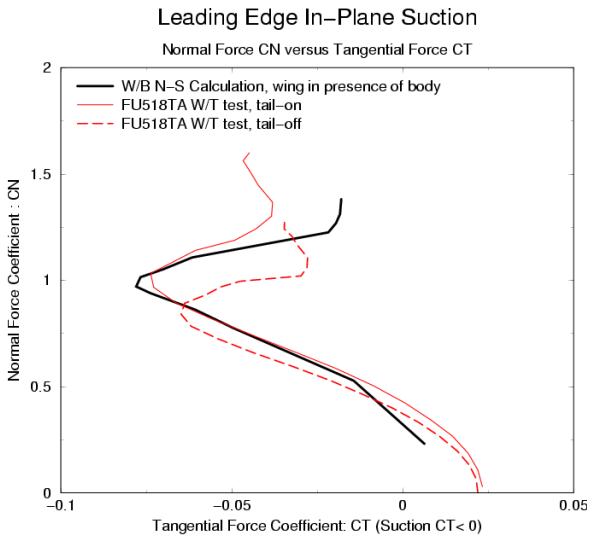

Fig 9. Comparison of Navier-Stokes computed CN(CT) with FU518TA W/T test data.

In the same way, computed tangential forces CT summed over the exposed part of the wing V0 were corrected and compared with measured tail-off data for FU518TA. CN versus CT is plotted in Fig 9. Suction breakdown is observed around CN=1.

In Fig 10, the pressure coefficient Cp versus the vertical coordinate Z is shown along a cut normal to the leading edge. The corrected AoA is 20 deg. Separation is reflected in the sudden local increase in pressure coefficient Cp illustrated on upper wing side (Z>0). At the leading edge suction peak, Mach numbers are locally all subsonic. The wing station at the beginning of the wing cut is at 58% half span.

Computed baseline V0 results, using the model of Fig 7, were not wholly compatible with the wind tunnel model. Corrections had to be made for different wing incidence (3 deg) and for boat tail effect. However, the overall qualitative agreement with the full configuration, including local disturbances on lift, was assumed fair enough for carrying on with the re-design using the simplified wing-body as background reference. Efforts should be concentrated on the outboard wing leading edge in front of 15% chord leaving the strake untouched.

As leading edge suction seems to be of decisive importance, the wing V0 should be the

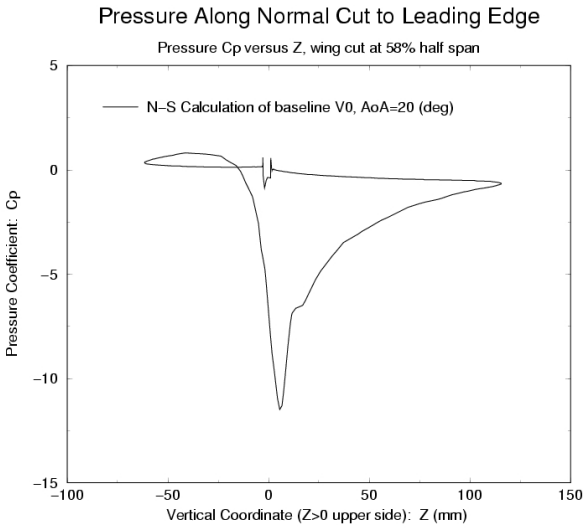

Fig 10. N-S calculated pressure Cp(Z), along cut perpendicular to the leading edge at 58% span.

reference for new designs. The study was to put emphasis on low speed characteristics with sparse outlook into transonic. To further restrict freedom, the wing plan form was to be the same as well as thickness and volume.

3 Strategy and Methods of Re-Design

3.1 Re-Design Procedure

Computational Fluid Dynamics (CFD) was applied on a large scale to improve on wing characteristics.

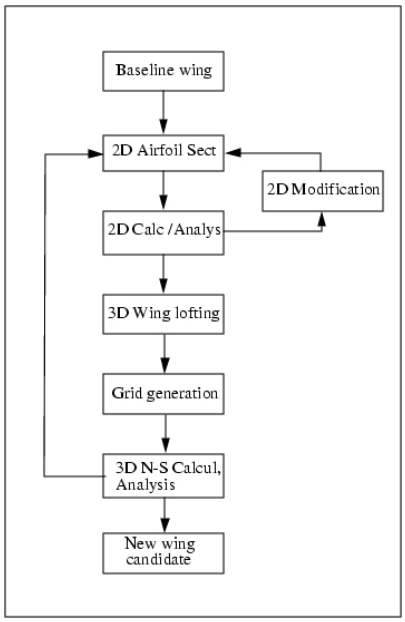

Fig 11. Re-design chart.

A classic design scheme, Fig 11, was set up based on an analogue 2D thinking for quick guidelines on how to change geometry in terms of nose droop and blow-up of nose thickness ahead of the 15 % chord line. Airfoil geometry perturbations were continuous up to second order derivative at the modification joint located at 15% wing chord. In combination with geometric leading edge measures, additional wing twist was considered. The simple model of Fig 7 was used for 3D assessments of design variations using 3D Navier-Stokes calculations.

Wing geometry modifications in a number of span stations were performed using a 2D airfoil geometry manipulation program PROFAN, Ref [2]. Once the 2D modifications were settled, the 3D wing lofting was carried out from modified 2D airfoils in a suitable number of wing sections. The lofting was performed using CATIA. 3D Navier-Stokes calculations were taken on using computational grids of hybrid type.

3.2 Methods

2D airfoil geometry manipulation is built on classic ideas by splitting up geometry into camber and thickness. These are distorted by additional perturbation functions. The method called PROFAN, Ref [2], was developed in-house for mission adaptive wing studies in the 80's. Leading or trailing edge deflections of camber line and local blow-up of leading edge thickness (as well as rigid twist rotation) can be performed with continuity in curvature at the specified re-design attachment location. The equivalent 2D flow analysis was carried out using MSES, a streamline curvature Euler code, Ref [3], with boundary layer of integral type. 3D surface lofting was performed in CATIA.

3D grid generation was carried out using the hybrid (tetrahedral/prismatic) ICEM CFD software. The 3D Naviers-Stokes (N-S) calculations were performed using the national 'EDGE' code, developed at FFA(FOI), Ref [4]. The turbulence model used was Wilcox standard k-ω. Reynolds' number based on aerodynamic mean chord was 3.4 million. No transition criterion was applied assuming turbulent flow all over. All N-S computations were executed on the in-house PC cluster called Maxwell using 14 parallel processors. One angle of attack took about 60-70 wall clock hours to converge using 3 multi-grid levels. The number of grid points was of order 3.4 million. About 9 angles of attack were calculated for each of the 7 different configurations. Hence about 4000 wall clock hours were spent in the computer cluster. In addition, several hundreds of 2D lift-drag polars were computed using the MSES code. Results were qualitatively assessed in low speed with sparse outlook into transonic.

4 Results

4.1 Geometry Modifications

Examples on treated 2D geometry modifications to the leading edge in a characteristic wing section (58% half span) can be seen in Figs 12-13. Wing alternative V2 is there compared with baseline V0.

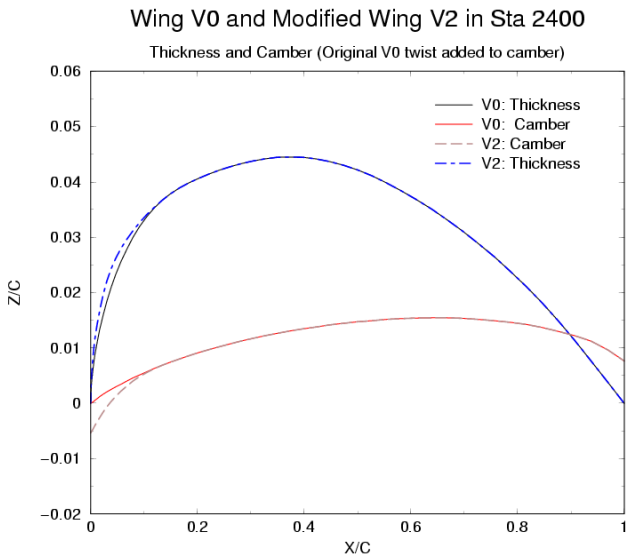

Fig 12. Camber nose droop (6 deg) and nose thickness blow-up (factor 1.4) in wing section.

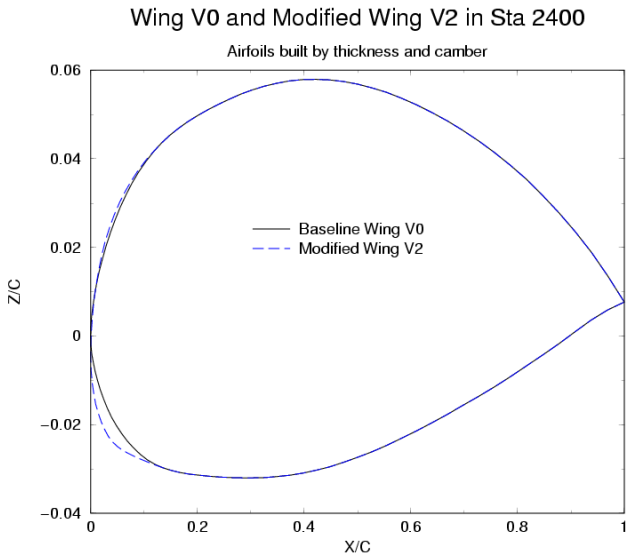

Fig 13. Built up airfoil having leading edge nose droop and nose thickness blow-up.

In Fig 14, the upper part is illustrating the lofted wing alternative V2 while the middle part is showing the kept plan form as well as one exception S2 in an attempt to investigate a leading edge extension (‘dog tooth’). However, the latter did not seem to perform substantially better than the original plan form. In the lower part of Fig 14, wing twist distributions are exemplified. The change in twist compared to baseline V0 is somewhat less than 0.5 degree for all treated cases. Baseline V0 has got 3 degrees washout at the wing tip compared to inboard incidence.

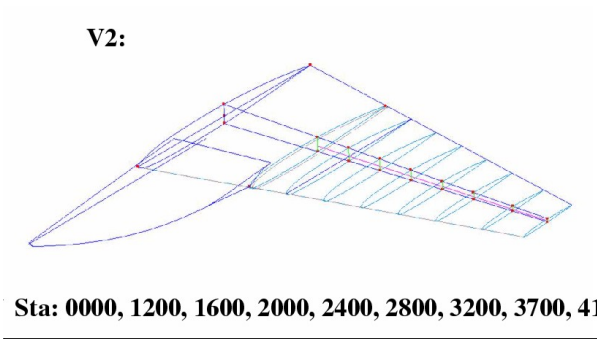

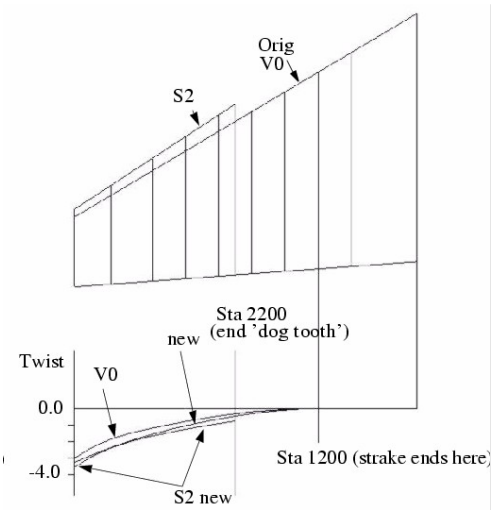

Fig 14. Lofted wing V2, wing plan forms and applied twist distributions.

Including the stretched leading edge extension (S2, Fig 14), 7 different wing versions were considered beside the baseline V0. A survey table of treated cases is found in Table 1. Table 1 reflects the gradual inclusion of more information by incorporating more airfoil sections to guide the lofting procedure. Too few sections resulted in local span-wise variations that could be quite strong e.g. like bulging out or shrinking of the nose contour in between given sections when gradually approaching the inner unchanged wing region. Most inclusion of section information is with the wing V5-25 and

Table 1. Survey of 3D lofted wing alternatives.

Wing ID	Nose deflect-ion (deg)	Nose Blow-up factor	Twist (id name / %C axis)	Remark
V0	-	-	Original V0	V0
V1-25	-	-	new/25%C	V0+modif
V1-50	-	-	new/50%C	V0+modif
V2	6	1.4-1.2	original V0	V0+modif
V3-25	6	1.4-1.2	new/25%C	V2+modif
V4-25	6	1.4-1.2	new/25%C	V3+modif
V5-25	6	1.4-1.2	new/25%C	V4+modif
S2	4	1.2	-	V2+lex (factor 1.11)

the stretched wing S2 ('dog tooth', see Fig 14) with 7 and 6 wing sections respectively.

All lofted cases were performed using CATIA with discrete point distributions derived in PROFAN. Original airfoil coordinates in a number of span wise sections were discretely extracted from the CAD model of the wing V0. Out of these airfoil coordinates, data were classically split up into camber and thickness providing input to the interactive PROFAN geometry manipulation code. After having processed this information in PROFAN making leading edge changes and checking results in 2D flow calculations, new section data were sent back to CATIA for creation of a new 3D wing for Navier-Stokes calculations, see Fig 11.

4.2 Importance of Leading Edge Suction

Equivalent 2D analysis in outer wing sections indicated very high suction peaks in the nose region, suggesting flow separation. In 3D this is an intricate mechanism as the inboard strake and the outboard wing are working together creating a highly 3D flow environment. Sudden flow changes are very likely to depend on small details of the wing and strake geometry. To avoid or delay outboard wing separation, changes in twist distribution and leading edge modifications became natural measures.

To illustrate this, the Cp distribution in one V5-25 wing section is shown in Fig 15.

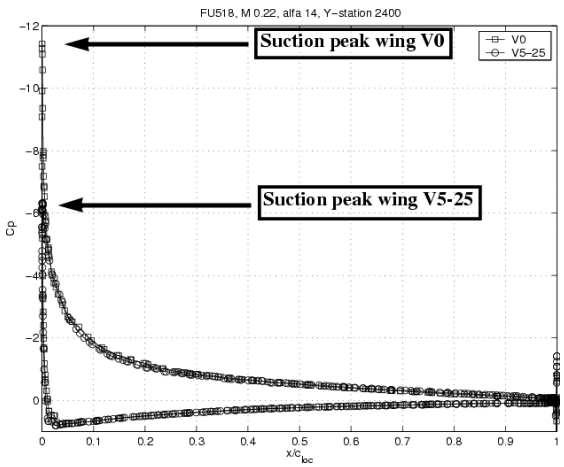

Fig 15. Suction peak comparison between wing V0 and V5-25 of 3D Navier-Stokes solutions.

A further illustration of outboard wing modifications can be seen in Fig 16. Here the pressure Cp is plotted against the vertical coordinate Z for V0 and V5-25 along a circumvented cut normal to the leading edge. In spite of the fact that the pressure peak is reduced (V5-25) the nose blow-up will yield a net gain of in-plane suction forces maintaining this to higher AoA. This is also demonstrated for all computed cases (Table 1) in Fig 17. The tangential force CT and normal force CN is summed over the wing and strake only. With increasing CN, the suction force (CT<0) increases until separation results in a decrease

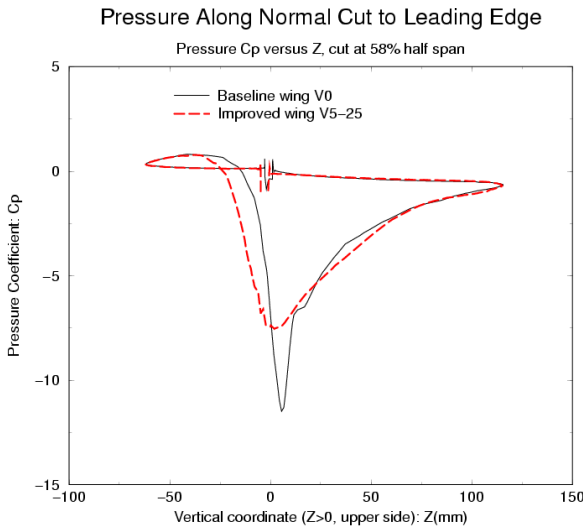

Fig 16. Pressure coefficient Cp of V0 and V5-25 in a cut perpendicular to the leading edge.

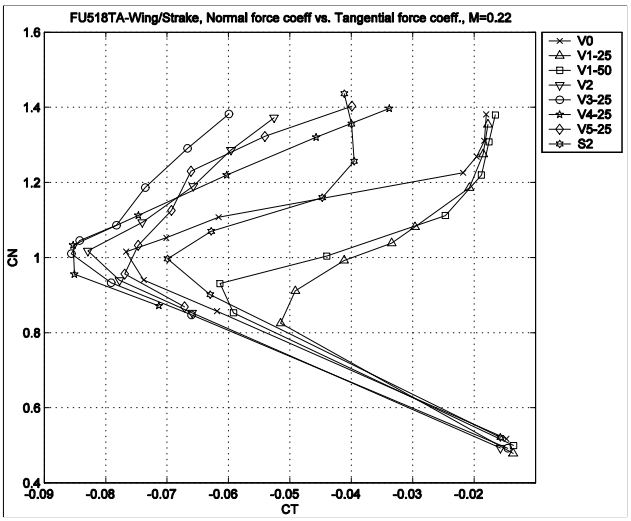

Fig17. In-plane suction forces (-CT) of wings.

and a gradual break down to fairly low suction levels. Although V0 has a high suction peak, it is degrading more rapidly than others not relieving the drag as much. The latter is demonstrated in Fig 18, where a comparison of drag between baseline V0 and V5-25 is shown. The drag of baseline V0 in Fig 18 is strikingly similar to that of the TWIG W/T model showing

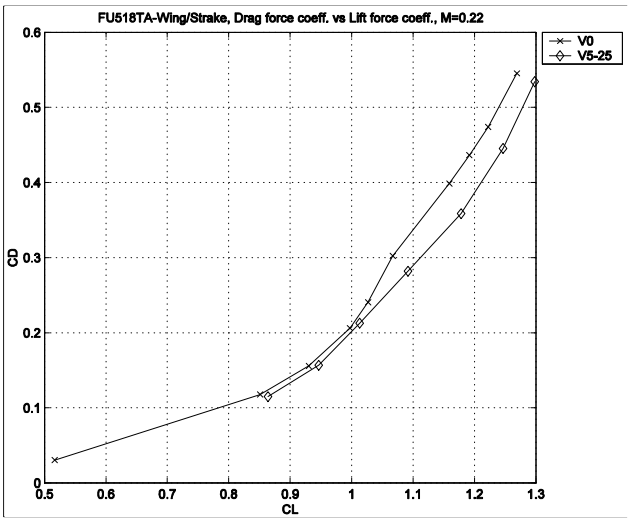

Fig 18. Drag CD(CL) of baseline V0 and wing V5-25. 3D N-S calculations at Mach 0.22.

the same type of 'glitch' as in Fig 6. In Fig 19 the corresponding comparison of lift is illustrated.

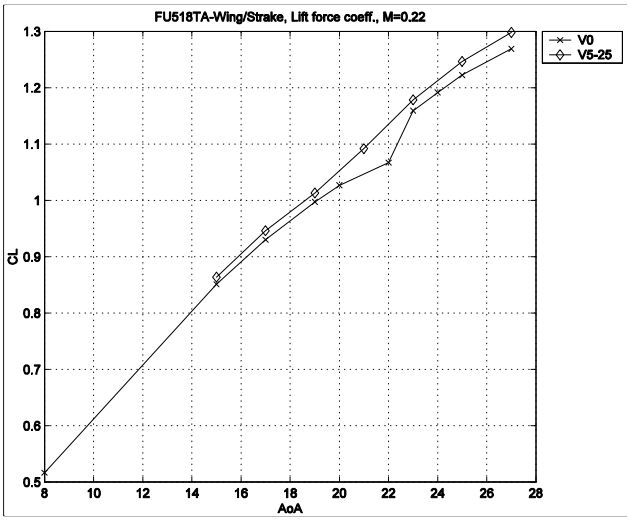

Fig 19. Lift vs AoA of wings V0 and V5-25. 3D N-S calculations at Mach 0.22.

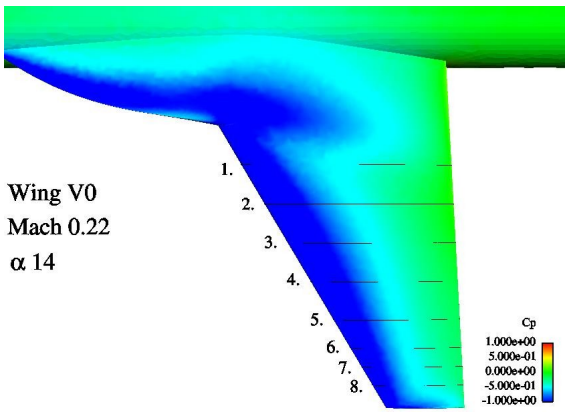

Fig 20. Upper surface wing pressure Cp of baseline V0 at Mach 0.22, AoA 14 degrees.

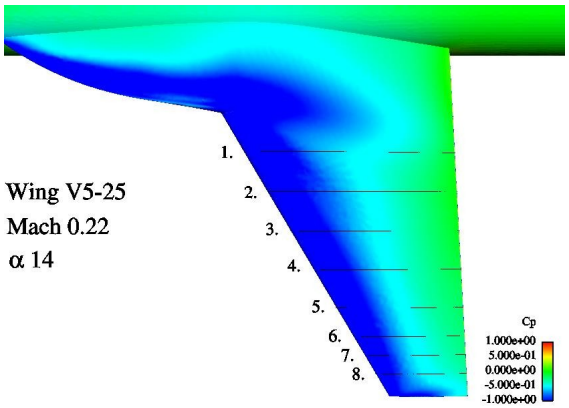

Fig 21. Upper surface pressure Cp of improved wing V5-25 at Mach 0.22, AoA 14 degrees.

4.3 Wing Pressure Distributions

Looking into Figs 20-21, comparing upper surface pressure Cp of the V5-25 wing with the baseline V0 at Mach 0.22 and AoA 14 degrees, there is not much of a difference overall. The differences are very local in the leading edge region as was shown earlier in Fig 15, showing chord-wise pressure Cp in wing section number 3. Similar trends are in other sections.

Generally, the peak suction ridge has been reduced by leading edge modifications of V5-25 and slightly changed wing twist. However, a net gain of in-plane suction forces have been obtained by the favorable balance between the increased forward facing leading edge front area and reduced leading edge suction Cp, resulting in delayed and smeared separation. This was also confirmed by details found in Figs 16-19.

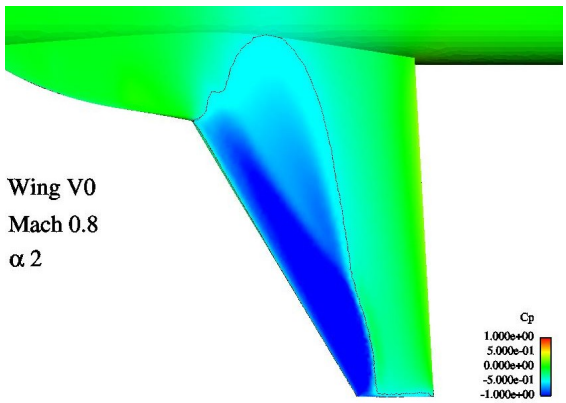

Fig 22. Upper surface pressure of baseline wing V0 at Mach 0.8, AoA 2 degrees.

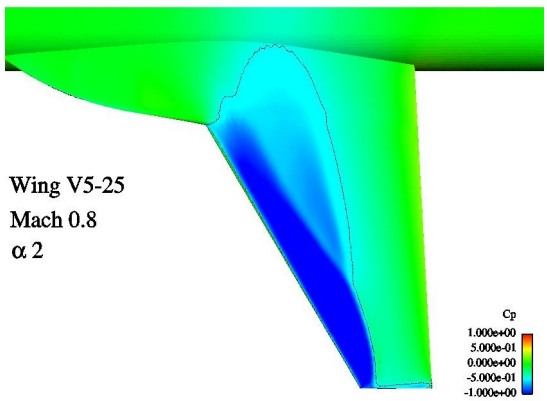

Fig 23. Upper surface pressure Cp of improved wing V5-25 at Mach 0.8, AoA 2 degrees.

Figs 22-23 show the same configurations in transonic at Mach 0.8 and AoA 2 degrees. In this case there are small but visual changes in pressure although they are not very pronounced. The sonic lines are indicated and seem practically to be almost in the same location.

In Figs 24-25, wing sections 2 and 5 (for locations see in Figs 20-21) are shown with comparison of pressure distributions in the chord-wise direction. Looking into some details, appearing recompressions on upper side are slightly moved upstream on wing V5-25. The tendency for an inboard lambda-type of swept back shock is a bit more pronounced with V5-25 due to the blow-up of leading edge thickness. The blow-up effect is also evident on the lower side. However, in the outboard wing part the re-compression shock seems to have somewhat weaker strength as compared to V0.

The wing re-design, focused in low speed

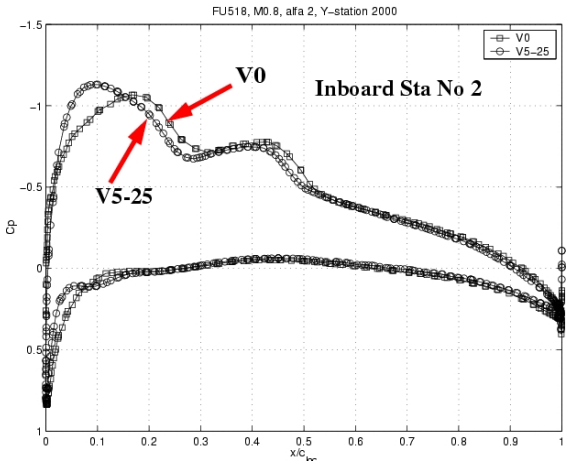

Fig 24. Pressure comparison in section No 2 of V0 and V5-25 at Mach 0.8 and AoA 2 degrees.

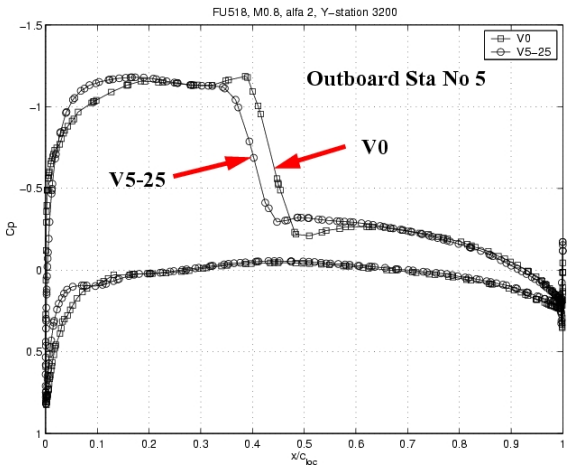

Fig 25. Pressure comparison in section No 5 of V0 and V5-25 at Mach 0.8 and AoA 2 degrees.

at high angles of attack, resulted in a reasonable design even in transonic at moderate CL-values. It was achieved by measures in the leading edge region and by small changes in twist. This was done with the same plan-form and maintained wing strake. Thickness and volume became the same as V0 behind 15% chord.

5 Concluding remarks

Computational analysis and re-design of a baseline wing-strake configuration using 3D Navier-Stokes calculations has been carried out. Investigation objectives of improvements of aerodynamic wing characteristics at high angles of attack were met. Conditions were set for keeping wing plan-form and shape of the strake intact allowing for outboard wing changes only.

A large number of modifications were computed. Measures taken were leading edge droop in combination with nose thickness blow-up with small changes in twist. Improvements were obtained in low speed high-lift conditions with minor differences in high-speed transonic. The idea was to improve on breakdown of leading edge suction delaying and smearing it. Improvements were achieved in lift and drag and 'glitch-like' behavior was reduced.

Acknowledgement

The senior author wants to thank his former GARTEUR GoR(AD) colleague Bram Elsenaar of NLR for stimulating discussions on 'glitches' and for making results available from Ref [1].

The authors are indebted to FMV (The Swedish Air Material Administration Board) for funding this work through NFFP (The Swedish National Program on Aeronautics Research and Development).

Finally, the authors want to thank our retired 'old hand' and much appreciated Saab colleague, former head of Geometry and Design, Pertti Skillermark, for his professional help by lofting all the wings.

References

[1] Rozendal D**.** Summary of experimental and theoretical wall interference investigation on the TWIG model in the HST and PHST wind tunnels. NLR-CR-2002-361.

[2] Sedin Y. ***'PROFAN'****:* An airfoil geometry- analysis and modification program. Internal Saab report L-0-1 B567, 1987. (In Swedish, title here translated.)

[3] Drela M. A User's Guide to MSES 2.5. MIT, 1993.

[4] Eliasson P. ***'EDGE'***, a Navier-Stokes solver for unstructured grids, Proc. to Finite Volumes for Complex Applications III, ISBN 1 9039 96341, pp. 527-534, 2002

[5] Hackström M., et al. NFFP-379: Configuration study-Trainer. Aerodynamic analysis. Saab Report FFE-2002-0018 (In Swedish, title translated).

[6] Sedin Y., et al. Aerodynamic wing design: Wing analysis using Navier-Stokes calculations on a wing-body combination with reference to improved wing characteristics of FU518TA. Saab Report FTA-2003-0064 .